Available online at www.sciencedirect.com

ScienceDirect

Geochimica et Cosmochimica Acta 121 (2013) 582–598

Geochimica et Cosmochimica Acta

www.elsevier.com/locate/gca

Redox effects on the microbial degradation of refractory organic matter in marine sediments

Clare E. Reimers [a,*], Yvan Alleau [a], James E. Bauer [b], Jennifer Delaney [c], Peter R. Girguis [c], Paul S. Schrader [a], Hilmar A. Stecher III [a,1]

[a] College of Earth, Ocean and Atmospheric Sciences, Oregon State University, 104 CEOAS Administration Building, Corvallis, OR 97331-5503, United States

[b] Aquatic Biogeochemistry Laboratory, Department of Evolution, Ecology, and Organismal Biology, Ohio State University, 318 W. 12th Avenue, Columbus, OH 43210-1293, United States

[c] Harvard University, Biological Laboratories, Room 3085, 16 Divinity Avenue, Cambridge, MA 02138-2020, United States

Received 22 March 2013; accepted in revised form 6 August 2013; available online 15 August 2013

Abstract

Microbially mediated reduction–oxidation (redox) reactions are often invoked as being the mechanisms by which redox state influences the degradation of sedimentary organic matter (OM) in the marine environment. To evaluate the effects of elevated, oscillating and reduced redox potentials on the fate of primarily aged, mineral-adsorbed OM contained in continental shelf sediments, we used microbial fuel cells to control redox state within and around marine sediments, without amending the sediments with reducing or oxidizing substances. We subsequently followed electron fluxes in the redox elevated and redox oscillating treatments, and related sediment chemical, isotopic and bacterial community changes to redox conditions over a 748-day experimental period.

The electron fluxes of the elevated and oscillating redox cells were consistent with models of organic carbon (OC) oxidation with time-dependent first-order rate constants declining from 0.023 to 0.005 y^{-1}, in agreement with rate constants derived from typical OC profiles and down core ages of offshore sediments, or from sulfate reduction rate measurements in similar sediments. Moreover, although cumulative electron fluxes were higher in the continuously elevated redox treatment, incremental rates of electron harvesting in the two treatments converged over the 2 year experiment. These similar rates were reflected in chemical indicators of OM metabolism such as dissolved OC and ammonia, and particulate OC concentrations, which were not significantly different among all treatments and controls over the experimental time-scale. In contrast, products of carbonate and opal dissolution and metal mobilization showed greater enrichments in sediments with elevated and oscillating redox states.

Microbial community composition in anode biofilms and surrounding sediments was assessed via high-throughput 16S rRNA gene sequencing, and these analyses revealed that the elevated and oscillatory redox treatments led to the enrichment of Deltaproteobacteria on the sediment-hosted anodes over time. Many Deltaproteobacteria are capable of using electrodes as terminal electron acceptors to completely oxidize organic substrates. Notably, Deltaproteobacteria were not measurably enriched in the sediments adjacent to anodes, suggesting that – in these experiments – electron-shuttling bacterial networks did not radiate out away from the electrodes, affecting millimeters or centimeters of sediment. Rather, microbial phylotypes allied to the Clostridia appeared to dominate in the sediment amongst all treatments, and likely played essential roles in converting complex dissolved and particulate sources of OM to simple fermentation products. Thus, we advance that the rate at which fermentation products are generated and migrate to oxidation fronts is what limits the remineralization of OM in many subsurface sediments removed from molecular oxygen. This is a diagenetic

* Corresponding author. Tel.: +1 541 737 2426; fax: +1 541 867 0220.
E-mail address: creimers@coas.oregonstate.edu (C.E. Reimers).
[1] Present address: Western Ecology Division, U.S. Environmental Protection Agency, Newport, OR 97365, United States.

http://dx.doi.org/10.1016/j.gca.2013.08.004

scenario that is consistent with the discharging behavior of redox oscillating sediment MFCs. It is also compatible with hypotheses that molecular O_2 – and not just the resulting elevated redox potential – may be required to effectively catalyze the degradation of refractory OM. Such decomposition reactions have been suggested to depend on substrate interactions with highly reactive oxygen-containing radicals and/or with specialized extracellular enzymes produced by aerobic prokaryotic or eukaryotic cells.

1. INTRODUCTION

Reduction–oxidation (redox) state is a chemical characteristic that influences early diagenesis and the burial of organic carbon (OC) in marine sediments. However, an exact microbial or chemical mechanism that explains redox mediation of sediment organic matter (OM) degradation, especially refractory OM remineralization, has not been identified definitively (Hartnett et al., 1998; Hedges et al., 1999). Sediment redox state is codependent with conditions such as deposition rate, OM flux, benthic faunal activities, and bottom water oxygen concentration. While deep-sea sediments may be oxic over tens to hundreds of meters depth (Røy et al., 2012), only exceptional near-shore sediments, such as in the Black Sea, are wholly anoxic due to deposition under a euxinic water-column (Canfield, 1993, 1994). The most geochemically complex sedimentary redox condition in the marine environment, found widely on continental margins, is an oscillating redox state that enhances benthic oxygen fluxes, alternately mobilizes and precipitates forms of iron and associated trace metals, and leads to little burial of reduced sulfur or OC (Aller, 1994, 1998; Forster and Graf, 1995; Morford and Emerson, 1999; McKee et al., 2004). The most common causes of sediment redox oscillation are macrofauna- and meiofauna-sediment interactions (i.e., bio-irrigation and bioturbation) (Aller et al., 2001). However, bed fluidization driven by periodic physical mixing events can also cause dramatic shifts in the redox state of estuarine and deltaic sediments, including the major tropical deltaic systems that are estimated to control the fate of ~60% of particulate organic matter injected by rivers or produced in the coastal ocean (Aller, 1998; Arzayus and Canuel, 2004; Aller et al., 2008). Thus, beds with redox oscillation may be of great significance as a source of respiratory CO_2 and other metabolic products, and they appear nearly as efficient in degrading complex forms of sedimentary OM as sediments that remain continually aerobic (Aller, 1998; Hulthe et al., 1998; McKee et al., 2004).

In general, the effect of positive redox conditions stemming from oxygen exposure on sediment OM degradation is a stimulation of hydrolysis and subsequent oxidation of more refractory OM pools over annual to millennial timescales (Keil et al., 1994; Thomson et al., 1998; Burdige, 2007). However, it is plausible that the redox state independently stimulates the degradation of more refractory OM, specifically via the energy benefits that elevated redox conditions provide to heterotrophic microbial communities, including those capable of extracellular electron transfer (EET). EET encompasses physiological processes by which certain microbes oxidize organic substrates (often simple organic acids such as acetate), transferring electrons in accordance with potential gradients to electron acceptors external to their outer cell membranes. EET was first recognized for its importance in dissimilatory mineral reduction by environmental microbiologists (Lovley and Phillips, 1988; Lovley and Chapelle, 1995; Nealson, 2010), but recent discoveries of EET through biofilms involving functionally diverse microorganisms are rapidly changing perceptions of its fundamental biogeochemical impact (Gorby et al., 2006; Reguera et al., 2005; Reimers et al., 2006; Rabaey et al., 2007; Marsili et al., 2008; Nielsen et al., 2009; Kiely et al., 2011). In several cultured Deltaproteobacteria, EET has been shown to occur through redox-active membrane-bound proteins such as a wide variety of *c*-type cytochromes acting as electrochemical gates, as well as through extracellular structures (referred to as pili or nanowires; Lovley, 2012). Another and more indirect mechanism of EET is through chemical carriers ("redox shuttles") including flavins, humic substances, and phenazines (Newman and Kolter, 2000; Rabaey et al., 2005, 2007; Marsili et al., 2008; Leung et al., 2011; Lovley, 2012).

EET in sediments may have the added consequence of separating sites of carbon metabolism from terminal electron acceptors. Thus, diverse communities may remineralize complex organic substrates by knitting together electrochemically conductive biofilms or by forming networks of filaments able to pass electrical currents through sediments and soils (Ishii et al., 2008; Nielsen et al., 2010; Risgaard-Petersen et al., 2012, and Pfeffer et al., 2012). Microbial fuel cells (MFCs) fueled with sediments appear to take advantage of long-range electron transport and regularly produce oxidation impacts extending out several centimeters from polarized anode surfaces (Tender et al., 2002; Ryckelynck et al., 2005). Not surprisingly, sediment MFCs as bioreactors have become an important research tool in studies of microbial ecology and biogeochemistry (Reimers et al., 2006, 2007; Rabaey et al., 2007; White et al., 2009).

In this paper we report the results of a unique 2-year long marine sediment microbial fuel cell incubation experiment designed to test the hypotheses that redox state selects for unique assemblages of heterotrophic bacteria, and that when exposed to elevated redox potentials, anaerobic microbes in marine sediments will enhance rates of OM degradation through electric coupling of spatially separated electrochemical half-reactions. The sediments selected for these experiments were recovered from subsurface layers of an open continental shelf environment and contained primarily aged, mineral-adsorbed, marine and terrestrial sources of OM that were expected to be resistant to anaerobic degradation and representative of typical hemipelagic sediments (Mayer, 1994). The experiments reported here eliminate consequences of direct oxygen exposure and fac-

tors such as disturbance, particle mixing, particle dispersal, and macro- or meio-faunal activities. The primary variable is redox potential, both fixed and oscillating, and the measured impacts are sediment biogeochemical constituents and bacterial community composition.

2. MATERIALS AND METHODS

2.1. Experimental setup

For this study, fine-grained, bioturbated sediments were sampled from 203 m water depth on the central Oregon shelf (43.92°N; 124.69°W) with a frame-mounted gravity corer. A bottom photo of the sampling location, in situ benthic fluxes, and O_2 microprofiles from this area of the Oregon shelf are presented in Berelson et al. (2013). In situ sediments are anoxic below 0.5 cm depth except at the boundaries of irrigated burrow structures. Total carbon degradation rates range from 7 to 17 mmol C m^{-2} d^{-1} but are largely driven by aerobic respiration, denitrification, and iron reduction in sediments <5 cm deep (Severmann et al., 2010; see pore water profiles in Supplementary material 1). Sedimentation rates, derived from excess ^{210}Pb profiles, equal approximately 0.1 cm/y (Wheatcroft et al., 2013).

To prepare homogenous anoxic sediment for four experimental treatments in triplicate, four cores (diameter 10.5 cm, sediment lengths 53–60 cm) were extruded under a N_2 atmosphere created in a glove bag. The uppermost ~5 cm of sediment was measured from the lowest level of surfaces that were often uneven, sectioned off, and discarded. Remaining sediment sections to 45 cm depth were retained in a plastic bucket. These subsurface muds were combined with 1.25 L of bottom seawater from the sample location that had been purged of O_2 by vigorous bubbling with N_2 gas. The sediments and bottom water were homogenized using a paint mixer spun by an electric drill. This mixing took place inside another glove bag under N_2. When thoroughly mixed, the sediments were repeatedly loaded into a plastic caulking gun and transferred to the experimental cells. These 12 cells consisted of an inner, lid-free, 250-mL Beckman polycarbonate centrifuge bottle. In three of the four sets of treatment bottles, four graphite rods were wired together to form a MFC anode (Fig. 1A); the fourth (control) treatment consisted of bottles with only sediment. Each anode rod was 8.2 cm long by 0.95 cm wide and was connected to the one copper conductor of a Type 4N5 neoprene covered cable (Pittsburgh Wire and Cable) with a ¾-inch 6–32 nylon screw capped with a 1-cm plug of water-resistant epoxy. The rods were drilled on the bottom, and seated over nylon screws projecting from a plastic base, to create an arrangement of one central rod surrounded by three others radiating out 1.9 cm and separated by 120°. The surface area of exposed graphite for each anode was therefore 98 cm^2, and the anodes occupied approximately 10% of the volume of the inner bottle. Sediments were added incrementally to each bottle, filling each about one third, tapping to expel N_2-gas space, moving to the next replicate bottle, repeating the process two times. Sediment splits were also saved in glass scintillation vials for subsequent "day-0" water content and solid phase analyses at each filling increment (see Section 2.3).

Once the inner centrifuge bottles were full, they were surrounded and covered uncapped, with the same homogenized sediment in 1 L open containers made from Nalgene HDPE bottles cut off just below the neck. These containers were submerged in seawater held in 4 L polypropylene beakers, and each sediment microbial fuel cell was completed by placing a 20 cm-long carbon-fiber brush cathode (Hasvold et al., 1997) and a reference electrode (Ag/AgCl [3 M KCl], Microelectrodes, Inc., MI-401F) in the outer beaker (Fig. 1B). The cathodes were pre-conditioned in seawater for 2 weeks prior to MFC assembly. All sediment manipulations and the set-up and maintenance of sediment MFCs took place in a shore-based laboratory cold room regulated to 11 ± 1 °C.

Throughout the experiment, aerated seawater was pumped continuously from a central reservoir through PVC piping and delivered serially to each cell by a computer-controlled system of 12 electromechanical relays (Measurement Computing USB_ERB24) and 12 VDC solenoid valves (Hayward model #SV10075STV12A/D) (Fig. 1C and D). Each seawater addition allowed flow for 6 s, displacing ~300 mL from around a single cathode. The displaced seawater then spilled out a side port in the cell's outer 4 L beaker and drained back through a return pipe to the central reservoir for re-aeration. A lag time of 36 s was programmed between each seawater addition down the line of cells (Fig. 1D), and the process ran continuously (except for occasions when the software halted and had to be restarted). The seawater in the reservoir was replaced every 1–2 weeks with fresh seawater obtained from the laboratory seawater system of the Hatfield Marine Science Center (HMSC), Newport, OR, USA. The Yaquina Bay source water for HMSC typically has salinities from 29–31, and it was passed through a sand filter and then a series of 20-, 5- and 1-μm cartridge filters prior to transfer to the experimental reservoir.

2.2. Redox control and electrochemical monitoring

The method of redox control used in these experiments was to poise anode potentials by regulating the potential difference between anode and cathode with individual custom-designed potentiostat circuit boards (NW Metasystems, Bainbridge Island, WA). Anodes, cathodes, and reference electrodes were wired through interconnected barrier strips located in the cold room and in an adjacent laboratory where the potentiostats were mounted on a wall (Fig. 1C). As will be shown, cathode potentials were relatively constant at 300–400 mV relative to Ag/AgCl (505–605 mV vs. NHE).

In the first of the treatments, the sediment-hosted electrodes were at "open circuit", which was always a negative potential due to the anoxic condition of the sediment. In a second treatment, anodes were held relatively positive (400 mV below the cathode potential) to simulate oxygen exposure. In the third treatment, the sediment-hosted electrode potentials were oscillated between relatively positive and negative states at 2-week (and after 518 days at 3-

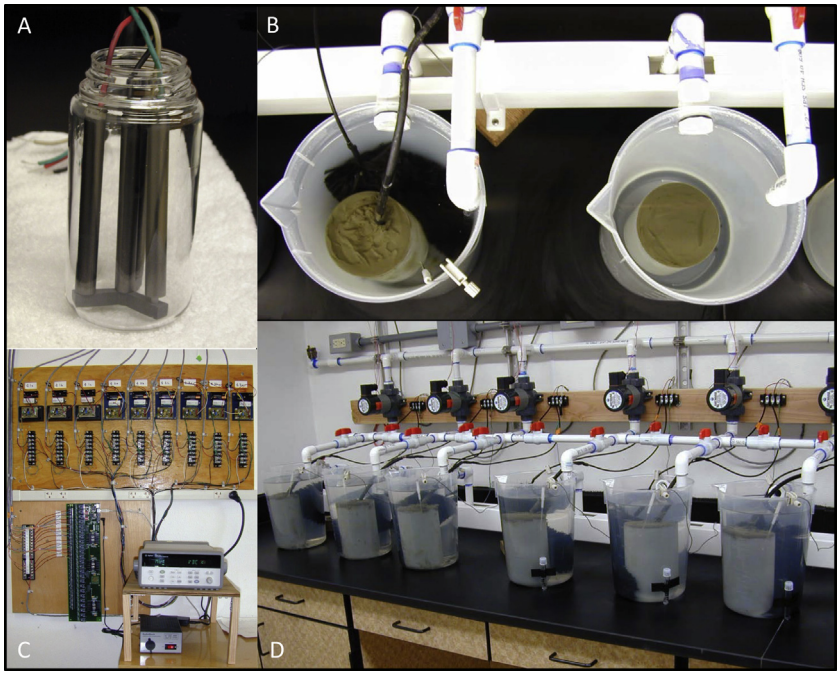

Fig. 1. Images of the experimental set-up. (A) Inner centrifuge bottle with anode array of four graphite rods. (B) Top-view of an assembled sediment microbial fuel cell (on left) and control (on right). Visible in back of the left cell is a cathode carbon-fiber brush and at the front of the cell is a small Ag/AgCl reference electrode. The top of cell's inner centrifuge bottle and anode rods are completely buried under >5 cm sediment. (C) Control room wiring of potentiostat load circuits (top), the electromechanical relay device for controlling the solenoid valves (lower left), and the multichannel datalogger (lower right). (D) Two sets of three experimental replicates showing the wiring of electrodes, and the seawater supply system valves and plumbing.

week) intervals. As a control for electrode exposure, the fourth treatment contained no electrodes but is presumed to have also been continuously negative.

Electrode potentials and the current flow in poised cells were monitored and recorded every 15 min with a multichannel datalogger (Agilent Technologies, Santa Clara, CA, model 34970A fitted with two 34901A multiplexer modules) wired to the potentiostat outputs (Fig. 1C). The current records were integrated over time to derive cumulative electron fluxes, and from these fluxes, estimates of carbon degradation rates.

2.3. Time-point sampling and chemical measurements

One replicate of each experimental treatment was sampled to characterize the pore water and solid sediment chemistry adjacent to the anodes and in the control after 99, 336, and 748 days of electrochemical monitoring. Initial (day-0) conditions were also assessed from four other companion 250 mL centrifuge bottles filled with homogenized sediment as the sediment MFCs were assembled. The subsequent sampling at the aforementioned timepoints involved transferring the 1 L containers of sediment from each selected MFC into a glove bag that was flushed and filled with N_2. The top 2–3 mm of sediment that had been directly in contact with aerated and regularly exchanged seawater was removed and saved in a glass scintillation vial. Next, the anode wires were cut as needed, and the inner centrifuge bottles of sediment were then extracted. These bottles were tightly capped under N_2 to prevent oxygen exposure, removed from the glove bag, cleaned off, and then centrifuged at 5000 rpm for 20 min in a temperature-regulated (10 °C) Sorvall centrifuge (as were the day-0 bottles). After centrifugation, the bottles were returned to the glove bag, opened, and the supernatant pore water was decanted into 125 mL trace metal clean HDPE bottles. Between 40 and 45 mL were immediately filtered through a 0.45 μm PTFE Gelman Acrodisc 25 mm syringe filter into another 125 mL trace metal clean HDPE bottle, and 30–45 mL were filtered through a pre-combusted 0.7 μm Whatman GF/F 25 mm disc filter into a pre-combusted glass flask. Aliquots of these filtrates were partitioned for chemical and isotopic analyses according to volumes and methods summarized in Table 1.

The sediment in each centrifuge bottle was also subsampled for microbial community composition analyses (see below), and the remainder frozen, then later freeze-dried and ground for chemical analyses. An exception to this procedure occurred with the day-748 samples. At this time point, three subsamples of ~25 g wet weight were removed from different locations within the mass of centrifuged sediment in order to evaluate chemical homogeneity. These three subsamples were stored in glass scintillation vials, later freeze-dried and ground, and analyzed discretely rather than as splits from one bulk sample.

Weight percent (wt.%) of total nitrogen (TN) and OC contents in dried sediments were determined in triplicate by high temperature combustion of 11–12 mg subsamples on a NC2500 ThermoQuest Elemental Analyzer (Hedges and Stern, 1984). Inorganic carbon was removed prior to

Table 1
Pore water processing and analytical procedures applied to time-series samples.

Analyte(s)	Filtering method	Volume allocated per subsample (mL)[a] (preservation method)	Pore water volume per analysis (mL)	Analytical precision ($\pm 1\sigma$)[b]	Analytical method
Total-H_2S	0.45 μm PTFE	1 (Fixed with 20 μL zinc acetate or analyzed immediately)	1	0.2 μM	Subsamples drawn under a N_2 atmosphere and mixed with diamine reagent concentration 'B' or 'C'; detected spectrophotometrically at 670 nm (after Cline, 1969)
TCO_2	0.45 μm PTFE	2.5 (Poisoned with 11 μl saturated $HgCl_2$ solution)	1	0.01 mM	CO_2 coulometer (UIC Inc., Coulometrics, Joliet, IL) with 1 mL sample loop
$\delta^{13}TCO_2$	0.45 μm PTFE	1 (Poisoned with 4.5 μL saturated $HgCl_2$ solution)	0.48	0.06‰	Measurements made on separate splits of the sample CO_2 using a Finnigan Delta V isotope ratio mass spectrometer
Fe, Mn	0.45 μm PTFE	1 (Acidified with 12 μL trace metal clean 3 M HCl)	0.6	0.8%	Samples mixed with 2.4 mL 1%HNO_3 and analyzed by Inductively Coupled Plasma-Optical Emission Spectroscopy
SO_4^{2-}, Cl^-	0.45 μm PTFE	1 (Refrigerated)	0.1	1%	Samples diluted 500× and analyzed by using a DX-500 ion chromatograph
Alkalinity	0.45 μm PTFE	2.5 (Poisoned with 11 μL saturated $HgCl_2$ solution)	2	0.1 mM	Gran titration using micro-burette
pH	Unfiltered	2 (Analyzed immediately)	2	n.d.	Glass pH electrode-NBS standards at 10 °C
Ammonia, Phosphate, Silicate	0.45 μm PTFE	3 (Frozen −50 °C)	Variable	Variable	After appropriate dilution of unacidified samples, analyses run on a nutrient autoanalyzer (Alpkem, Clackmas, OR)
Dissolved OC	0.7 μm GF/F	5 (Mixed with 63 μL H_3PO_4)	0.1	6 μM	High-temperature oxidation with a Pt catalyst, utilizing a Shimadzu TOC-5000A analyzer
$\delta^{13}DOC$	0.7 μm GF/F	15 (Frozen −50 °C)	10–15	0.7‰	The procedure for extracting CO_2 from dissolved OC for $\delta^{13}C$ analyses is described in detail by Raymond and Bauer (2001) and Bauer and Bianchi (2011). The CO_2 was collected in 6 mm OD Pyrex tubes and analyzed using a Finnigan Delta Plus IV isotope ratio mass spectrometer (IRMS)

[a] Triplicate aliquots were retained except for $\delta^{13}DOC$.
[b] Estimated from true replicate determinations of samples and standards; n.d. = not determined.

OC analysis by acid fumigation, whereas TN contents were determined from unacidified samples. The average standard deviation of TN and OC analyses was 0.004 and 0.03 wt.%, respectively. Analytical repeatability (Caulcutt and Boddy, 1983) was assessed by rerunning samples (years apart) with different standards and found to match the precision of replicates within single runs. Splits of bulk dried sediments were also analyzed for concentrations of total reduced inorganic sulfur using the chromium reduction method (Canfield et al., 1986) in the laboratory of T. Lyons (University of California Riverside). The average standard deviation of S analyses was 0.04 wt.%.

The stable isotopic composition of particulate OC was measured by isotope ratio mass spectrometry using a CarloErba 1500 Elemental Analyzer coupled to a ThermoQuest Deltaplus XP Mass Spectrometer after acidification and drying of the sediment samples (Hatten et al., 2012). Stable isotope results are reported using standard δ notation to express $^{13}C/^{12}C$ ratios of the samples relative to the v-PDB standard. The average standard deviation of triplicate stable isotope measurements of particulate OC was 0.2‰.

2.4. Microbial DNA extraction

Anodes from each individual time point and treatment were stored in Whirl-Pak bags (Nasco, Ft. Atkinson, WI) at −50 °C and later sampled by scraping their graphite surfaces using a sterilized razor blade. The scrapings were collected, weighed and placed in microcentrifuge tubes. Total genomic DNA was extracted using the Power Soil DNA Isolation Kit (MoBio Laboratories, Carlsbad, CA) following the manufacturer's protocol with the added cell lysis procedure consisting of heating the sample to 60 °C followed by three cycles of intermittent bead beating for 60 s and chilling on ice for 60 s. Total genomic DNA from sediment subsamples (0.3 g taken from random locations within the centrifuged bulk material surrounding the anodes and temporarily stored at −50 °C) was similarly extracted. DNA was collected and stored in 10 mM Tris. Each DNA sample was quantified using Quant-IT dsDNA HS Assay Kit and Qubit fluorometer (Invitrogen, Eugene, OR). Total extracted DNA from each sample ranged from 50 to 850 ng.

2.5. Microbial community determinations

DNA amplification and sequencing was performed by the Research and Testing Laboratory (Lubbock, TX). 16S rRNA genes were amplified by PCR using 28F (5′-GA GTT TGA TCM TGG CTC AG-3′) and 519R (5′-GWA TTA CCG CGG CKG CTG-3′) primers (Nielsen et al., 2008), which are designed to target bacterial and not eukaryotic or archaeal communities. Amplicons were sequenced using 454 pyrosequencing (454 Life Sciences, Branford, CT) (Margulies et al., 2005) and Titanium reagent chemistry. Raw sequences were processed, quality filtered, and analyzed using the QIIME 1.4.0 software package (Caporaso et al., 2010). Sequences were clustered at 97% similarity with USEARCH (Edgar, 2010), and the most abundant sequence was chosen as representative for each operational taxonomic unit (OTU). Chimera detection was conducted using UCHIME, and only those sequences flagged as non-chimeras by both *de novo* and reference-based (Gold database) methods were retained for further analyses (Edgar et al., 2011). Taxonomic assignments were made using the Ribosomal Database Project (RDP) classifier (Wang et al., 2007). A subsamples of abundant OTUs not successfully classified with RDP were subsequently identified using Basic Local Alignment Search Tool (BLAST;Altschul et al., 1990).

3. RESULTS AND DISCUSSION

3.1. Electrochemical records

In this study, the redox potentials of open-system sediment incubations were controlled for over 2 years via graphite electrodes and potentiostats. By utilizing an array of four evenly spaced anode rods, all volumes of incubated sediment were within 2 cm of an anode surface. The different redox potentials are documented in Fig. 2A, which also shows that the electrochemical measurements of replicate cells were nearly identical leading up to time points when individual cells were sacrificed for sediment chemistry and microbiological characterizations. The "open circuit" treatment always exhibited redox potentials less than −0.4 V (vs. Ag/AgCl), which is indicative of consistent anoxic conditions poised by the sulfate/sulfide redox couple (Berner, 1963). The redox elevated treatment varied between −0.12 and 0.036 V (vs. Ag/AgCl) with a mean redox potential of −0.032 ±0.038 (1 SD; vs. Ag/AgCl). As the offset between anode and cathode was fixed to simulate a constant oxygen exposure, the observed variability was driven by cathode potential changes in response to exchanges of seawater and likely changes in the biofilms on the cathode carbon fibers. The oscillating redox treatment was set to oscillate between the conditions of the open circuit and redox elevated treatments at 2 week (and later 3 week) intervals, and was also affected by cathode potential shifts due to aforementioned reasons. Over time, the anode potentials during open circuit intervals of the oscillating cells progressively increased and it took longer for these potentials to decline to minimum values (Fig. 2A). This indicates an oxidized zone grew in around the anodes and that it took increasingly longer to replenish this zone with reduced chemical species through diffusive transport or microbial regeneration.

Fig. 2B shows the current harvested from the MFCs of redox elevated and redox oscillating treatments, and Fig. 2C displays the cumulative electron flux derived from the current records. A pronounced peak in current was observed over the first 60 days in the redox elevated treatment

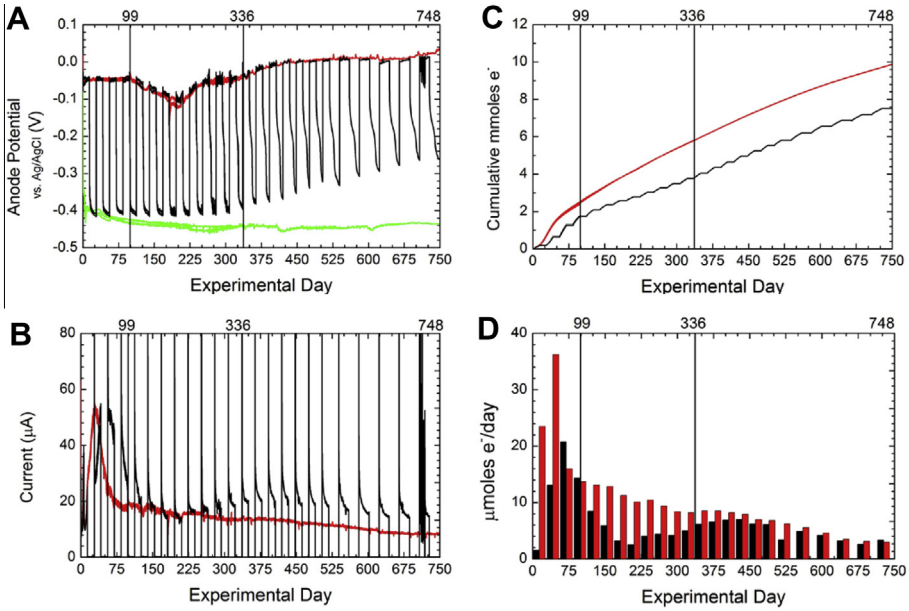

Fig. 2. Time-series of (A) anode potential and (B) current in sediment treatments with anodes. Green, red and black records are from open circuit, redox elevated, and redox oscillating treatments, respectively, and they show triplicate records until sediment microbial fuel cells were sampled at 99 days, duplicate to 336 days, and single remaining cell records to 748 days. Representations of current as cumulative electron flux are shown in (C), and these fluxes are converted to block-average rates of electron harvesting over the duration of each full redox cycle in (D).

record (for all three replicates), but this peak was delayed and repeatedly interrupted by the oscillation cycle applied to the third treatment which started with a closed circuit interval. After 60 days, the continuously harvested current of the redox elevated treatment cells declined gradually, while currents during closed circuit intervals of the oscillating treatment increased to higher baseline levels (Fig. 2B). Each new period of elevated redox potential started with a current spike followed by an exponential decline consistent with a potential step response modeled after an RC circuit (Bard and Faulkner, 2001; Dewan et al., 2009). This behavior is consistent with previous studies of sediment MFCs in which potential was oscillated over time (Gardel et al., 2012). This behavior is also consistent with the ability of some electrode-hosted biofilms to store electrical charge resulting from the oxidation of organic substrates (Uría et al., 2011). Within the second year of the experiment, the overall rate of electrons harvested by the oscillating cells was nearly equivalent to the continuously redox elevated cells. This suggests the electron flux in both treatments became similarly limited by the production rate of substrate(s) (e.g., acetate) or terminal respiration products (e.g., sulfide) that can be supplied by diffusion to – or from within – the anode biofilm. Fig. 2D displays block averages of these rates calculated for consecutive oscillation periods.

3.2. Rates of carbon remineralization

If we interpret the current harvested by the sediment microbial fuel cells to be a dynamic measurement of electrons derived from anaerobic transformation products of sediment OM (Brüchert and Arnosti, 2003), we have a novel method to assess OC remineralization rates and rate constants for the continental margin sediments in this study. Our approach starts with a well-known model in geochemistry (Middelburg, 1989; Canfield, 1993) by which we assume that total OM is oxidized according to first-order kinetics:

$$\frac{dG_T}{dt} = -k(t)G_T \tag{1}$$

Herein, G_T is the total mass of OC contained in each centrifuge bottle and k is a time-dependent first-order rate parameter. We then estimate k for discrete time intervals, Δt, as:

$$k = \frac{1}{\Delta t}\ln\frac{G_t}{G_{(t+\Delta t)}} \tag{2}$$

where G_t is the OC at successive times throughout the experiment that may be estimated from the cumulative electron flux $\sum e^-$ at t (Fig. 2C) as

$$G_t = G_o - \left(\frac{\sum e^-}{4} * \frac{0.012}{\alpha}\right). \tag{3}$$

In expression (3), explicit units are required such that G_o is the initial OC content of the sediment in grams, $\sum e^-$ at t is in mmoles, and a is a unitless coulombic efficiency factor. The electron flux is divided by 4 because we assume $CH_2O(\text{organic matter}) + 2H_2O = HCO_3^- + 5H^+ + 4e^-$, and the stoichiometry is the same whether electrons are derived directly from organic substrates or from secondary OM remineralization products (e.g., H_2S) produced during the incubations. We have estimated G_o as equal to 2.9 ± 0.2 gC per replicate from determinations of the particulate OC in day-0 sediments (1.59 ± 0.02 wt.% dry sediment), the sediment water content (45 ± 2 wt.%), an estimate that each treatment bottle with anodes contained 220 cm^3 of wet sediment, and average grain densities equated to 2.5 g cm^{-3}. We do not have a measure of a, but past studies with different configurations of MFCs and different organic substrates suggest $0.1 < a < 0.7$ (Liu et al., 2005; Reimers et al., 2007; Jung and Regan, 2007). Factors that would reduce a are bacterial utilization of natural electron acceptors in the sediments in place of the anodes and substrate utilization diverted into biomass growth (Logan et al., 2006). Conversely a could be elevated by the oxidation of iron sulfides present in the sediments at the start of the incubations. We have assumed a equal to 0.6 and acknowledge it could have varied, especially early in the incubations. Measurements such as isotopic composition of various carbon pools and pore water iron and sulfide inventories, discussed below, do independently integrate the effects of all mineralization processes we attempt to account for with the efficiency factor a.

Notably, when the results of the redox elevated and redox oscillating experiments are used to calculate k for successive time intervals (as in Fig. 2D), we find $k = 0.023$–0.005 y^{-1} in good agreement with typical rate constants derived for offshore subsurface sediments from OC profiles and down core ages (Middelburg, 1989). The corresponding remineralization rates are low (0.01–0.07 μmol C $cm^{-3}d^{-1}$) compared to rates derived from incubation or diagenetic modeling studies evaluating surface sediments containing sources of labile OM (e.g., Soetaert et al., 1996; Hulthe et al., 1998). However, these rates are of the same order of magnitude as carbon remineralization rates inferred from ^{35}S-labeled sulfate reduction rate measurements from other subsurface sediments, for example on the Washington continental margin at 100 m (Hartnett and Devol, 2003). This implies that our efficiency assumptions are likely representative and that the experiments succeeded in mimicking natural conditions controlling the remineralization of refractory sedimentary OM buried below the zone of bioturbation. The finding that rates for redox elevated and redox oscillating treatments also converge suggests that these two redox conditions should have similar effects on long term carbon burial.

3.3. Sediment OC pools over time

The rate determinations presented above predict a total loss of OC after 2 years equal to less than two percent of G_o for the bulk sediment of the redox elevated and oscillating treatments. As corroboration and to make comparisons between all experimental redox conditions, OC concentrations and isotopic ratios in dissolved and solid-phase OM pools are presented in panels A–D of Fig. 3 by time point for all treatments and the control. In contrast, Fig. 3E por-

trays particulate OC concentrations from the surface 2–3 mm of sediment fully exposed to oxygenated seawater above the inner cells.

All treatments exhibited a sharp decrease in dissolved OC pools between day-0 and day-99 (Fig. 3A) with accompanying shifts in the $\delta^{13}C$ of the residual dissolved OC (Fig. 3B). The first 99 days of the experiment coincided with the highest electron fluxes in the redox elevated and oscillating treatments (Fig. 2D), however, the pore water data do not point to an effect of redox condition on rates of dissolved OC consumption or production. By day-748, the residual dissolved OC appears to be dominated primarily by ^{13}C-depleted substrates except in the control (Fig. 3B). A relationship between the isotopic values of pore water OC and concentrations demonstrates the preferential consumption of relatively ^{13}C-enriched dissolved OC biochemical fractions through remineralization reactions leaving behind lighter presumably less reactive forms of dissolved OC that are possibly of terrestrial origin, e.g., lignin (Fig. 4A). The inference behind Fig. 4A (a plot based on an isotopic mass balance model for two-component mixtures) is that the slope of any linear segment linking data points gives a direct estimate of the isotopic value of the component undergoing progressive reaction (Aller and Blair, 2006). A similar plot for TCO_2 (Fig. 4B) can reveal what OC sources are being actively remineralized, and/or if dissolved inorganic carbon is added through $CaCO_3$ dissolution.

The decrease in dissolved OC pools alone (~2.5 mmol/L * 0.1 L or 0.25 mmoles OC, Fig. 3A) is insufficient to support the cumulative electron fluxes of the redox elevated and oscillating cells (Fig. 2C). The remainder of the cumulative electron flux may therefore result from addition and subsequent oxidation of hydrolysis products generated from particulate OM. The total cumulative electron fluxes predict that the particulate OC concentrations in these treatments should have declined by ~0.03 wt.% between day-0 and day-748. Fig. 3C shows that instead, particulate OC concentrations increased by 0.06–0.14 wt.% over time in all treatments, which are changes that are greater than the average analytical precision of the measurements (0.03 wt.%). If grouped by time, these changes are significant based on Friedman ANOVA nonparametric tests at the 0.05 significance level. If grouped by treatment, the

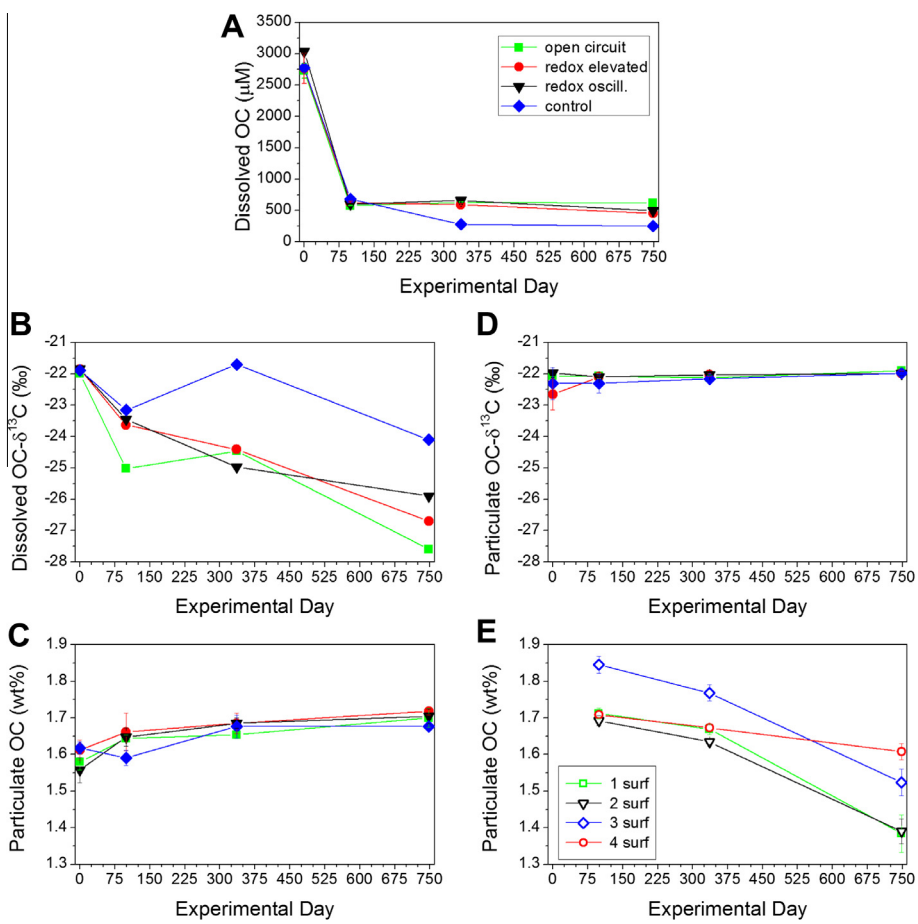

Fig. 3. (A) Dissolved OC concentrations, (B) dissolved OC–$\delta^{13}C$, (C) particulate OC as percent dry weight of sediment, and (D) particulate OC–$\delta^{13}C$ at four time points (0, 99, 336 and 748 days) for incubated sediments according to redox treatment. (E) Particulate OC content of surface sediment exposed to oxic seawater in the experimental cells (as seen in Fig. 1B) over three sampling time points. Vertical error bars (often smaller than symbol sizes) represent ± 1 SD about the mean of analyses of triplicate samples. Dissolved OC–$\delta^{13}C$ analyses were not replicated due to insufficient sample volume.

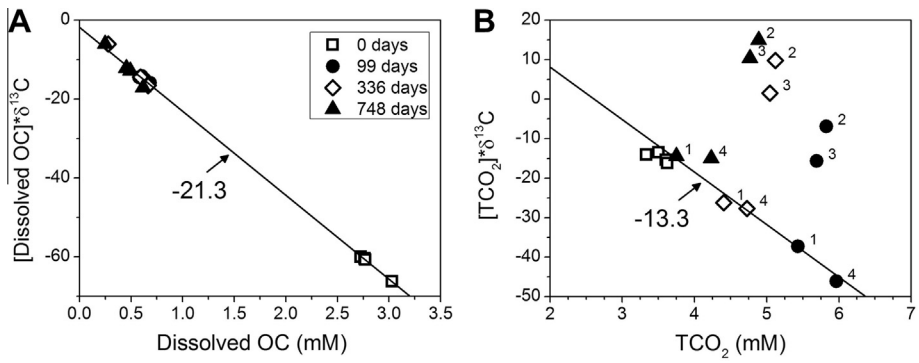

Fig. 4. (A) The relationship between pore water dissolved OC concentrations and corresponding products of dissolved OC concentrations and isotopic ratios over time. The slope of −21.3‰ demonstrates a higher loss of substrates with less negative isotopic values (e.g., typical marine OC with $\delta^{13}C = -20‰$ to $-21‰$) compared to terrestrial substrates ($\delta^{13}C = -26‰$ to $-27‰$) (Hastings et al., 2012) during incubation. (B) The relationship between pore water inorganic carbon (TCO_2) concentrations and corresponding products of dissolved inorganic carbon concentrations and isotopic ratios over time. Point labels indicate treatment (1-open circuit, 2-redox elevated, 3-redox oscillating, 4-control) and help to show that the pore water TCO_2 of the redox-elevated and oscillating treatments became progressively enriched in ^{13}C.

different redox conditions have statistically indistinguishable effects on particulate OC concentration (again at the 0.05 significance level). Furthermore, the method of subsampling the particulate pools (random subsamples versus splits of homogenized bulk material) did not affect the variability of particulate OC analyses. Analyses of discrete subsamples taken at day-748 are no more heterogeneous than replicated bulk sample analyses at day-99 or day-336 (see Section 2.3).

Cumulative losses of 4–8% of the total sediment mass due to dissolution of inorganic constituents can explain the observed rises in particulate OC wt.%. Evidence for time-progressive losses of $CaCO_3$ and opal affecting all treatments is discussed below and could feasibly produce the apparent OC enrichments. Alternatively, particulate OC could have been enriched through chemoautotrophic productivity (see feasibility calculations in Supplementary material 2), which would generate particulate and dissolved OC from dissolved inorganic carbon and the oxidation of reduced chemical species, primarily sulfide. However, we are of the opinion that an OC enrichment from chemoautotrophy of the magnitude observed would be improbable in light of insufficient sulfide in the sediments for energy generation (as it was low to undetectable in the treatments as discussed in more detail below). Moreover, the trends observed in the phylogenetic assessments do not reflect a dominance of known chemoautotrophs in the sediment communities (see Section 3.4 and Supplementary material 3). Although, there is the possibility that uncharacterized archaea may have been prominent autotrophs in these anoxic sediments.

Particulate OC isotopic ratios (Fig. 3D) and TN:OC ratios remained statistically unchanged from day-0 to day-748 as did total reduced S:OC (data not shown). These results indicate that remineralization (or the aforementioned potential chemoautrophy) processes during the incubations had proportionally small impacts on these bulk particulate pools. The TN:OC ratios were between 0.091 and 0.096 (mol:mol) which Hastings et al. (2012) show is characteristic of Oregon mid-shelf muds containing marine and vascular plant OM sources. S:OC ratios ranged from 0.16 to 0.18 (mol/mol). This is also within the typical range for most fine-grained marine siliciclastic sediments (Morse and Berner, 1995).

Lastly, the very surface sediments that were exposed to agitated, fully aerated seawater in all treatments throughout the experiment declined in particulate OC content from day-0 to day-748 (Fig. 3E). Friedman ANOVA nonparametric tests at the 0.05 significance level again conclude differences between time points are significant; however, surface-sediment particulate OC contents decrease with time while the bulk incubated sediment particulate OC concentrations increase. The surface samples were not otherwise characterized, and we do not wish to over interpret particulate OC concentrations confounded by compound effects of OM degradation, possible chemoautotrophy and inorganic mineral dissolution/precipitation. However, differences between the sediment OC concentrations of the incubated and surface samples at day-748 were from 0.11 to 0.32 wt.%. The consistently lower surface values suggest that direct exposure to molecular oxygen leads to faster OM decomposition than exposure to an elevated redox state created by poising electrodes alone.

3.4. Open system effects of redox on inorganic pore water constituents

One of the fundamental conditions influencing early diagenetic processes is the open system character of near surface sediments. Within and below the zone of irrigation and bioturbation, diffusion acts to counterbalance the net production or consumption of dissolved metabolites and regulates local microbial and equilibrium processes. A defining feature of the sediment MFC incubations reported here is that these were open systems allowing diffusive coupling of anaerobic sediments to a sediment–water interface

above, as well as to embedded redox-regulated anodes. Mean diffusion times for most pore water constituents over distances of ~10 cm are 40–130 days at 10 °C (Jørgensen, 2006). Thus, time series of pore water inorganic constituents reflect the interplay between redox-modulated early-diagenetic reactions, diffusion and the microorganisms responsible for catalyzing OM oxidation.

As has already been shown, electron fluxes stemming from OM oxidation were greatest early in redox elevated and oscillating treatments, and this is reflected in increases in TCO_2 and ammonia at day-99 (Fig. 5A and C). However, open circuit and control treatments show initial increases in TCO_2 and ammonia that bracket the others. These results indicate anaerobic respiration was comparable in all treatments. It is also apparent that respiration rates declined in all treatments over time, allowing diffusive exchange to erode TCO_2 and ammonia concentrations.

Inorganic chemical species tied to S, Fe, and Mn cycling differed across the treatments. Redox elevated or oscillating treatments contained little to no detectable total-H_2S at day-99, -336 and -748 (Fig. 5D). In addition, SO_4^{2-}/Cl^- ratios in pore water increased over time to near seawater ratios suggesting greater net sulfate retention or production compared to open circuit or control treatments (Fig. 5E). Dissolved iron and manganese (presumably as Fe(II) and Mn(II)) were elevated in redox elevated and oscillating treatments (Fig. 6A and B), which also showed accentuated phosphate losses (Fig. 6C). The uptake of phosphate by adsorption and precipitation reactions at redox-elevated anode surfaces has been observed in previous sediment MFC studies (Ryckelynck et al., 2005).

Consequences of proton or proton-equivalent production are apparent in the time series of redox elevated and oscillating treatments. By day-336 and -748, the bulk pore water pH of the redox elevated treatment < redox oscillating treatment < open circuit treatment < control (Fig. 6D) which also appears to have influenced pore water Mn concentrations (Fig. 6B). In addition, TCO_2–$\delta^{13}C$ values shift positive in cells with elevated redox conditions (Fig. 5B) and deviate abruptly from strict respiratory control. Fig. 4B indicates pore water TCO_2 concentrations and isotopic ratios within reduced redox treatments were likely controlled by the respiration of marine OC (~−20‰; Hastings et al., 2012) modulated by differential diffusive exchanges of ^{13}C-inorganic carbon species with overlying waters (McNichol et al., 1988) and minor amounts of carbonate dissolution. In contrast, TCO_2 concentrations in redox-elevated or oscillating treatments reflected greater

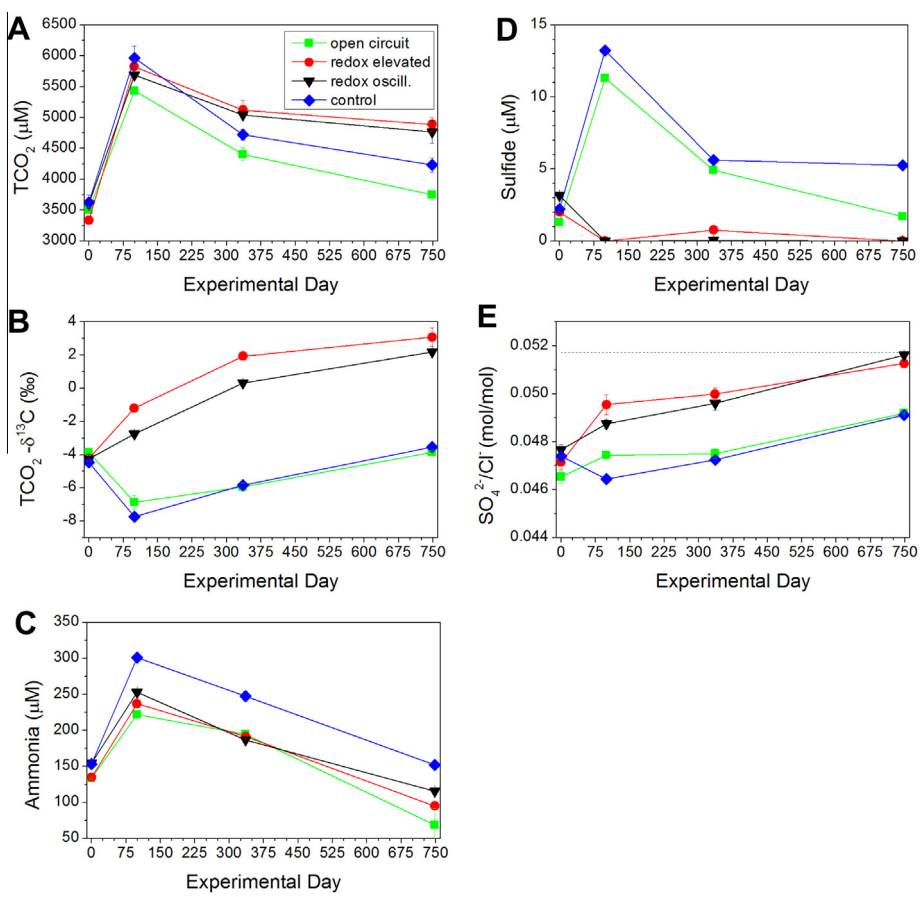

Fig. 5. The variability of pore water (A) TCO_2, (B) TCO_2–$\delta^{13}C$, (C) ammonia, (D) sulfide and (E) SO_4^{2-}/Cl^- at four time points according to treatment. Vertical error bars represent ± 1 SD about the mean of analyses of triplicate samples. In (E) the dotted horizontal line represents the stoichiometric ratio of average seawater.

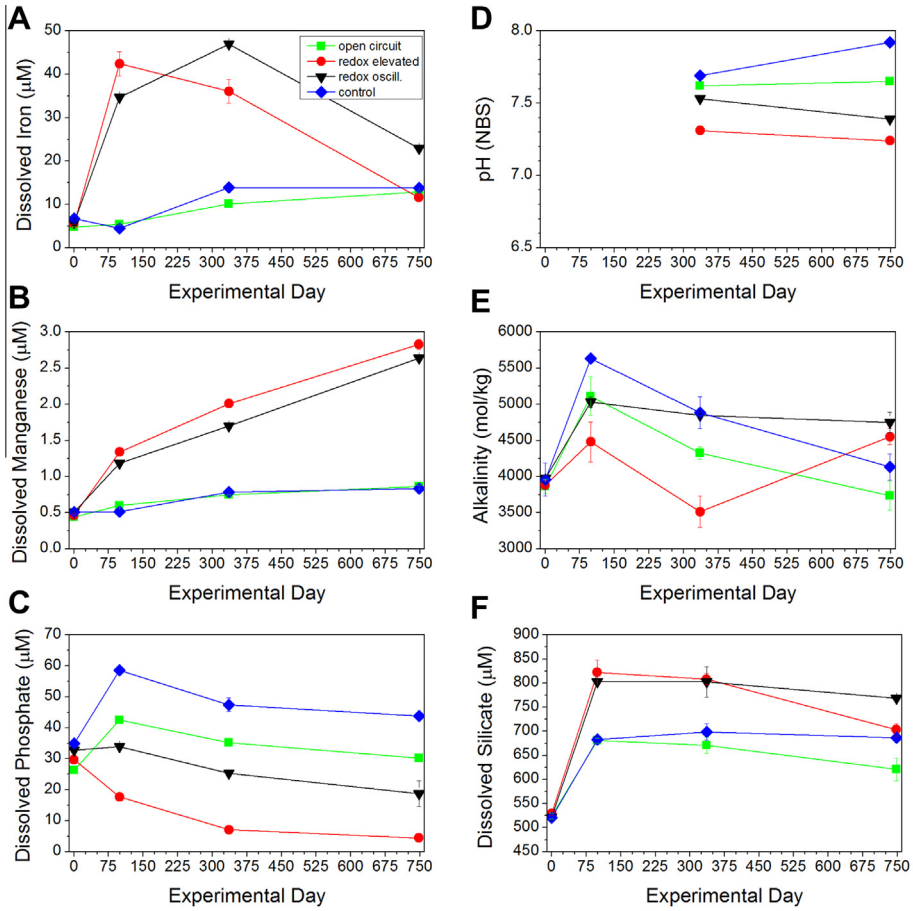

Fig. 6. The variability of pore water concentrations of (A) iron, (B) manganese, (C) phosphate, (D) pH, (E) total alkalinity, and F) silicate at four time points according to treatment. Vertical error bars represent ± 1 SD about the mean of analyses of triplicate samples. pH measurements were made as single determinations only, in the pore waters collected at 336 and 748 days.

admixtures of inorganic carbon derived directly from the dissolution of sediment carbonates (enriched in ^{13}C). Alkalinity (Fig. 6E) did not build up steadily, because of diffusive exchanges, and because of reactive losses coupled to production of acid during the oxidation of sulfides, iron and other anaerobic metabolites, especially in the redox-elevated cells (Aller, 1982; Boudreau and Canfield, 1993). Dissolved silicate accumulated and was maintained above day-0 values, especially in redox elevated and oscillating treatments, in spite of diffusive exchange. These trends are evidence of opal dissolution throughout the experiment, which along with $CaCO_3$ dissolution and minor FeS losses, could explain the small time-progressive increases in %OC (provided initial concentrations of these phases were at least 10% of the starting sediment; see Section 3.2, Fig. 3C).

3.5. Bacterial community analyses of sediments and anode biofilms

Analyses of the 16S rRNA gene sequences of DNA extracted from the four redox treatments at day-0 to day-748 time points suggest that biofilms adhering to anodes developed distinct enrichments, whereas microbial communities in the bulk sediment samples were more similar over the course of the experiment amongst all treatments (Figs. 7 and 8). Proportions of bacterial sequences at the class level are illustrated to show changing dominance, however proportions to the order level are reported as Supplementary material 3. At day-0, the four parallel characterizations of homogenized starting sediments show a high degree of similarity (Fig. 7) which implies reproducible starting conditions and methodologies. In the day-0 samples, 59–62% of bacterial sequences were unclassified, which declined to 24–39% in later time-series samples. BLAST analyses indicated that the most abundant of the unclassified sequences were allied at the 99% level to other unclassified bacterium clones reported from Pacific Ocean margin sediments (e.g., clone: C9001C_B01_1_C006 from subseafloor sediments off Shimokita Peninsula; Kobayashi et al., 2008). Frequently observed and classifiable sequences in both anode and sediment samples included members of the phylum Firmicutes (class Clostridia), the phylum Chloroflexi (class Anaerolineae), as well as Fusobacteria, Deltaproteobacteria, and Gammaproteobacteria. Clostridia-like phylotypes in

Fig. 7. Time-series class level representation of dominant bacteria sequences in incubated sediment samples by treatment. Emphasized are ribotypes that exceeded 5% dominance in one or more sample.

sediment samples peaked at day-99, when electron fluxes were highest amongst the discrete sample points (Fig. 7). Clostridia are generally characterized as obligate anaerobes able to produce low molecular weight fermentation products from complex organic substrates. In sediments and wastewater, *Clostridium* spp. produce organic acids such as lactate and acetate that are utilized by sulfate reducing bacteria, typically allied to genera of Deltaproteobacteria (Zhao et al., 2008; Guerrero-Barajas et al., 2011). In this study, Deltaproteobacteria enrichments of redox elevated anode samples were as high as 59% at day-99, and Gammaproteobacteria comprised as much as 67–69% of reads from anodes from the open circuit treatment (day-336) and the redox oscillating treatment (day-748) (Fig. 8). Deltaproteobacteria also comprised 7–20% of the total bacterial 16S rRNA genes in the sediments regardless of time or treatment (Fig. 7). The dominant Deltaproteobacterial sequences were primarily allied to the obligately anaerobic sulfate/sulfur reducers, Desulfobacterales and Desulfuromonales. The dominant Gammaproteobacteria sequences

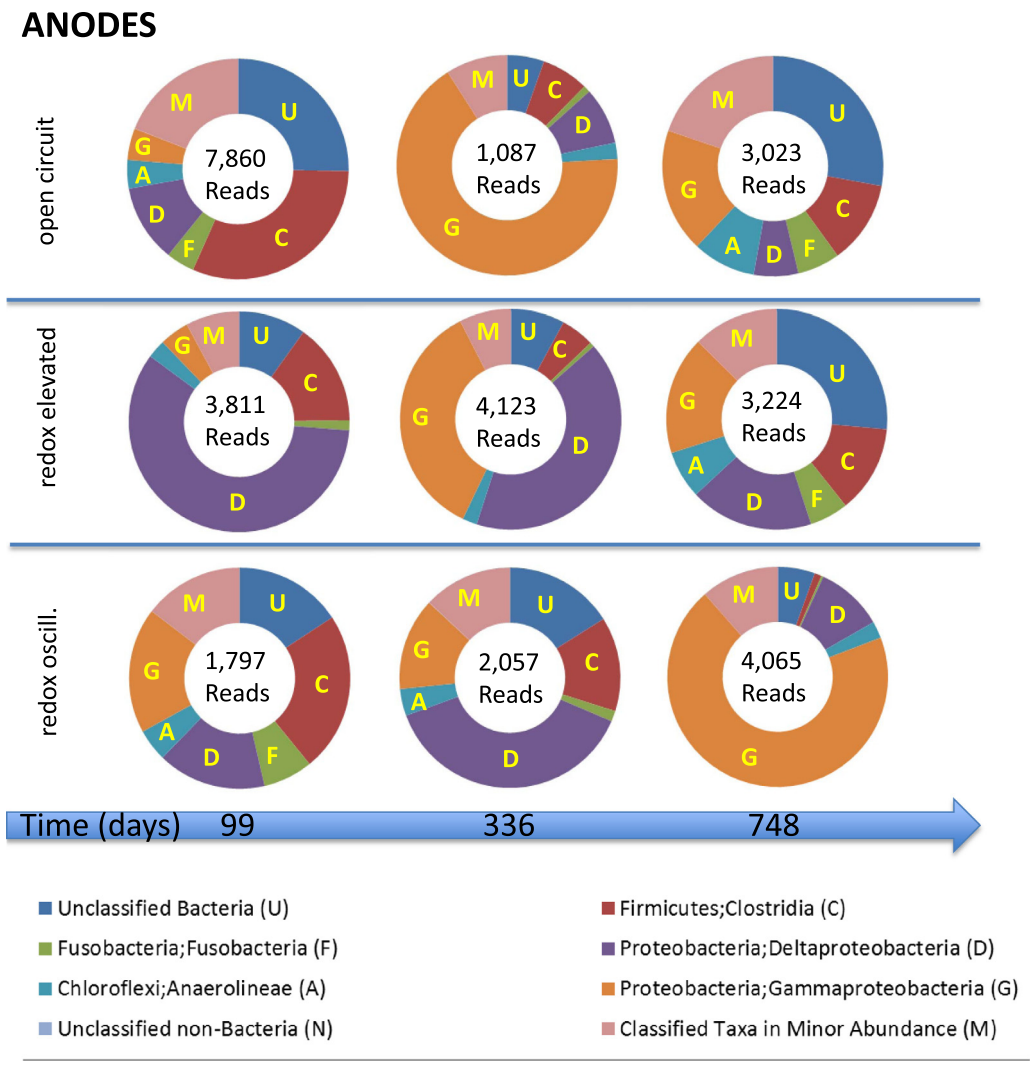

Fig. 8. Time-series class level representation of dominant bacteria sequences in anode biofilm samples by treatment.

aligned with Oceanospirillales. When found in anoxic sediments, Oceanospirillales and Anaerolineae-related bacteria have been described as chemoorganotrophs capable of hydrolyzing biopolymers, or respiring organic compounds with NO_3^- or other electron acceptors (Rusch et al., 2009; Blazejak and Schippers, 2010). Other uncultured Gammaproteobacteria found in highly sulfidic tidal sediments have been described as having chemolithoautotrphic metabolism based on sulfur oxidation (Lenk et al., 2011, Supplementary material 2).

4. IMPLICATIONS

The coupling of biogeochemical reactions across redox zones after episodes of redox oscillation has been invoked to explain dissolution of iron sulfides and calcium carbonates in marine sediments (Nielsen et al., 2010; Risgaard-Petersen et al., 2012), and hypothesized to promote OM remineralization (Aller, 1994) via bacteria capable of EET (Nielsen et al., 2010). In this study, electrodes in contact with sediments and maintained at -0.032 ± 0.038 V (vs. Ag/AgCl) created a redox state sufficiently oxidizing to simulate oxygen exposure and to promote extracellular electron transfer by the microorganisms known for establishing electrical connections within sediments; i.e., model strains of Deltaproteobacteria (Lovley, 2012). More specifically, *Geobacter sulfurreducens,* have been shown to generate electric currents centered at -0.29 V (vs. Ag/AgCl) while completely oxidizing acetate (Srikantha et al., 2007)[2]. Deltaproteobacteria are frequently enriched on anodes within sediment MFCs (Holmes et al., 2004; Reimers et al., 2006), and include strains that grow anaerobically, oxidizing a variety of fermentation products with concomitant reduction of iron oxides, elemental sulfur, or humic substances. *G. sulfurreducens* produce pili networks that would seem able to promote long-range electron transport

[2] Srikantha et al. (2007) present cyclic voltammetry of immobilized *Geobacter sulfurreducens* on graphite electrodes. Their results reveal maximum currents centered at -.29V (vs. Ag/AgCl) within voltage scans.

through sediments (Lovley, 2012), and Desulfobulbaceae include filamentous bacteria which function as electron transporters over centimeter scales (Pfeffer et al., 2012). We therefore expected, over 2-year experiments, to detect greater Deltaproteobacteria enrichments and greater rates of OM remineralization under redox-elevated and redox-oscillating conditions compared to sediments with highly reduced redox conditions. The essence of the hypotheses tested were that the amount of energy gained from passing electrons to terminal electron acceptors influences rates of OC remineralization, and that bacteria capable of EET, working in concert with syntrophic partners, would promote OM degradation.

However, the experimental results do not show geochemical evidence for either redox conditions (as established in this study) or the observed Deltaproteobacteria enrichments at redox-elevated boundaries, influencing remineralization rates of sediment OC. With no transport mechanisms active other than diffusion, pore water indicators of OM metabolism such as dissolved OC, and ammonia were very similar among treatments. This finding is in contrast to previous studies in which direct oxygen exposure maintained at 100% of air saturation produced sediment OC oxidation rates of 0.070–0.125 μmol C cm^{-3} d^{-1} that were up to 3.5-fold greater than rates with the same sediments under anoxic conditions (Hulthe et al., 1998).

The rates of OC oxidation inferred from the electron fluxes measured in this study were lower (0.01–0.07 μmol C cm^{-3} d^{-1}) than rates commonly observed in near-surface sediments, but consistent with model- or sulfate reduction rate-estimates of OC losses from anaerobic subsurface sediments. The debate over redox effects has often centered on relatively refractory OM preserved when anaerobic sediments are permanently buried. These same organic substrates are lost from layers such as uppermost turbidite sequences or mobile bed deposits, re-exposed to oxygen (Prahl et al., 1997; Aller, 1998; Thomson et al., 1998). The present study suggests that redox elevation and/or oscillation alone does not remove the bottleneck limiting anaerobic respiration. Redox coupling does result in dissolution of iron sulfides and carbonates in anoxic layers of sediment, but these processes and conditions appear unable to catalyze essential heterotrophic activities to the same extent as direct exposure to dissolved molecular O_2. This conclusion is supported by comparative particulate OC measurements between the sediments incubated anaerobically in contact with MFC anodes and overlying sediments in direct contact with aerated seawater (Fig. 3C vs. E).

Another implication is that biochemical rather than energy-based explanations for a redox connection to rates of sedimentary OM remineralization may be required to explain the observed patterns in the present study. One such explanation is that aerobic decomposition may be uniquely aided by the generation of highly reactive oxygen-containing radicals that work with extracellular enzymes produced only by aerobic prokaryotic cells, or metazoans with flow-through guts, to break bonds and depolymerize the most refractory organic compounds such as lignin or cellulose as a pre-condition for metabolism (Canfield, 1994; Mayer et al., 2001; Sun et al., 2002; Bianchi, 2011). Alternatively, any O_2 exposure may lead to production and accumulation of bacterial or meiofaunal biomass, and the subsequent destruction of this biomass after a redox shift may prime suboxic remineralization (Aller, 1994; Aller et al., 2001; Hee et al., 2001; Bianchi, 2011). Likewise, the greater number and diversity of organisms that graze upon bacteria in oxic compared to anoxic sediments has been suggested to explain higher rates of carbon remineralization (or decomposition) under oxygen exposure (Lee, 1992).

Finally, observations that electron fluxes – and by inference rates of terminal metabolism – converged for redox-elevated and redox-oscillating treatments, and that the latter treatment illustrated a capacitive buildup of electron donors and double exponential decay curves of anode potential during late open circuit periods (Fig. 2A) may provide additional insights into the consequences of redox zonation. The decay curves suggest two sources of reductants supplying anode surfaces. The electron donors were likely in the form of inorganic metabolites such as hydrogen sulfide, and slower diffusing low molecular weight organic substrates that the bacterial community could only oxidize at locales of elevated potential. Thus, the diffusive supply of fermentation products to bacteria populating redox-elevated zones may ultimately regulate subsurface OC remineralization when redox gradients are present.

If highly reducing redox conditions persisted for decades to millennia in one layer of sediment compared to another with a downward penetrating redox gradient, as in the difference between surficial- and bottom-turbidite lithologies (Thomson et al., 1998), then carbon preservation differences could emerge from rate differences too small to detect in solid phase or pore water characterizations over most laboratory time scales. Confirming this conjecture will continue to prove difficult. This study points to examining further the turnover of fermentation products and the microbial agents active along spatially expanded sedimentary redox gradients.

ACKNOWLEDGMENTS

The authors gratefully acknowledge contributions to the experimental maintenance and analytical work in this study by J. Jennings, K. Howell, C. Doolan, M. Nielsen, and E. Keesee. The sediments were collected during cruise W0506A from the R/V *Wecoma*. Shiptime and the experimental set-up were supported under National Science Foundation grant OCE02-42048. Microbial community analyses and manuscript preparation were supported with funds from the Office of Naval Research, Award Number: N000140910199 to CER. The thoughtful suggestions of three anonymous reviewers and associate editor E. Canuel helped to improve the presentation of this work.

APPENDIX A. SUPPLEMENTARY DATA

Supplementary data associated with this article can be found, in the online version, at http://dx.doi.org/10.1016/j.gca.2013.08.004.

REFERENCES

Aller R. C. (1982) Carbonate dissolution in nearshore terrigenous muds: the role of physical and biological reworking. *J. Geol.* **90**, 79–95.

Aller R. C. (1994) Bioturbation and remineralization of sedimentary organic matter: effects of redox oscillation. *Chem. Geol.* **114**, 331–345.

Aller R. C. (1998) Mobile deltaic and continental shelf muds as suboxic, fluidized bed reactors. *Mar. Chem.* **61**, 143–155.

Aller R. C., Aller J. Y. and Kemp P. F. (2001) Effects of particle and solute transport on rates and extent of remineralization in bioturbated sediments. In *Organism–Sediment Interactions* (eds. J. Y. Aller, S. A. Woodin and R. C. Aller). University of South Carolina Press, pp. 315–333.

Aller R. C., Blair N. E. and Brunskill G. J. (2008) Early diagenetic cycling, incineration, and burial of sedimentary organic C in the central Gulf of Papua (Papua New Guinea). *J. Geophys. Res.* **113**, F01S09. http://dx.doi.org/10.1029/2006JF000689.

Aller R. C. and Blair N. E. (2006) Carbon remineralization in the Amazon–Guianas tropical mobile mudbelt: a sedimentary incinerator. *Cont. Shelf Res.* **26**, 2241–2259.

Altschul S. F., Gish W., Miller W., Myers E. W. and Lipman D. J. (1990) Basic Local Alignment Search Tool. . *Mol. Biol.* **215**, 403–410.

Arzayus K. M. and Canuel E. A. (2004) Organic matter degradation in sediments of the York River estuary: effects of biological vs. physical mixing. *Geochim. Cosmochim. Acta* **69**(2), 455–463.

Bard A. J. and Faulkner L. R. (2001) *Electrochemical Methods*. John Wiley & Sons, Inc., New York.

Bauer J. E. and Bianchi T. S. (2011) Dissolved organic carbon cycling and transformation. In *Treatise on Estuarine and Coastal Science, Biogeochemistry*, vol. 5 (eds. E. Wolanski and D. S. McLusky). Academic Press, Waltham, pp. 7–67.

Berelson W., McManus J., Severmann S. and Reimers C. E. (2013) Benthic flux of oxygen and nutrients across Oregon/California shelf sediments. *Cont. Shelf Res.* **55**, 66–75.

Berner R. A. (1963) Electrode studies of hydrogen sulfide in marine sediments. *Geochim. Cosmochim. Acta* **27**, 563–575.

Bianchi T. (2011) The role of terrestrially derived organic carbon in the coastal ocean: a changing paradigm and the priming effect. *PNAS* **108**, 19473–19481.

Blazejak A. and Schippers A. (2010) High abundance of JS-1- and Chloroflexi-related bacteria in deeply buried marine sediments revealed by quantitative, real-time PCR. *FEMS Microbiol. Ecol.* **72**, 198–207.

Boudreau B. P. and Canfield D. E. (1993) A comparison of closed- and open-system models for porewater pH and calcite-saturation state. *Geochim. Cosmochim. Acta* **57**, 317–334.

Brüchert V. and Arnosti C. (2003) Anaerobic carbon transformation:experimental studies with flow-through cells. *Mar. Chem.* **80**, 171–183.

Burdige D. J. (2007) Preservation of organic matter in marine sediments: controls, mechanisms, and an imbalance in sediment organic carbon budgets? *Chem. Rev.* **107**, 467–485.

Canfield D. E. (1993) Organic matter oxidation in marine sediments. In *Interactions of C, N, P and S Biogeochemical Cycles and Global Change* (eds. R. Wollast, F. T. Mackenzie and L. Chou). Springer-Verlag, Berlin, pp. 333–363.

Canfield D. E. (1994) Factors influencing organic carbon preservation in marine sediments. *Chem. Geol.* **114**, 315–329.

Canfield D. E., Raiswell R., Westrich J. T., Reaves C. M. and Berner R. A. (1986) The use of chromium reduction in the analysis of reduced inorganic sulfur in sediments and shales. *Chem. Geol.* **54**, 149–155.

Caporaso J. G., Kuczynski J., Stombaugh J., Bittinger K., Bushman F. D., Costello E. K., Fierer N., Gonzalez P. A., Goodrich J. K., Gordon J. I., Huttley G. A., Kelley S. T., Knights D., Koenig J. E., Ley R. E., Lozupone C. A., McDonald D., Muegge B. D., Pirrung M., Reeder J., Sevinsky J. R., Turnbaugh P. J., Walters W. A., Widmann J., Yatsunenko T., Zaneveld J. and Knight R. (2010) QIIME allows analysis of high-throughput community sequencing data. *Nat. Methods* **7**(5), 335–336.

Caulcutt R. and Boddy R. (1983) *Statistics for Analytical Chemists*. Chapman & Hall/CRC, New York.

Cline J. D. (1969) Spectrophotometric determination of hydrogen sulfide in natural waters. *Limnol. Oceanogr.* **14**, 454–458.

Dewan A., Bekenal H. and Lewandowski Z. (2009) Intermittent energy harvesting improves the performance of microbial fuel cells. *Environ. Sci. Technol.* **43**, 4600–4605.

Edgar R. C. (2010) Search and clustering orders of magnitude faster than BLAST. *Bioinformatics* **26**(19), 2460–2461.

Edgar R. C., Haas B. J., Clemente J. C., Quince C. and Knight R. (2011) UCHIME improves sensitivity and speed of chimera detection. *Bioinformatics* **27**, 2194–2200.

Forster S. and Graf G. (1995) Impact of irrigation on oxygen flux into the sediment: intermittent pumping by *Callianassa subterranea* and "piston pumping" by *Lanice conchilega*. *Mar. Biol.* **123**, 246–335.

Gardel E. J., Nielsen M. E., Grisdela, Jr., P. T. and Girguis P. R. (2012) Duty cycling influences current generation in multi-anode environmental microbial fuel cells. *Environ. Sci. Technol.* **46**, 5222–5229.

Gorby Y. A., Yanina S., McLean J. S., Rosso K. M., Moyles D., Dohnalkova A., Beveridge T. J., Chang I. S., Kim B. H., Kim K. S., Culley D. E., Reed S. B., Romine M. F., Saffarini D. A., Hill E. A., Shi L., Elias D. A., Kennedy D. W., Pinchuk G., Watanabe K., Ishii S., Logan B., Nealson K. H. and Fredrickson J. K. (2006) Electrically conductive bacterial nanowires produced by *Shewanella oneidensis* strain MR-1 and other microorganisms. *PNAS* **103**, 11358–11363.

Guerrero-Barajas C., Garibay-Orijel C. and Rosas-Rocha L. E. (2011) Sulfate reduction and trichloroethylene biodegradation by a marine microbial community from hydrothermal vent sediments. *Int. Biodeterior. Biodegrad.* **65**, 116–123.

Hatten J. A., Goñi M. A. and Wheatcroft R. A. (2012) Chemical characteristics of particulate organic matter from a small, mountainous river system in the Oregon Coast Range, USA. *Biogeochemistry* **107**, 43–66.

Hartnett H. E. and Devol A. H. (2003) Role of a strong oxygen-deficient zone in the preservation and degradation of organic matter: a carbon budget for the continental margins of northwest Mexico and Washington State. *Geochim. Cosmochim. Acta* **67**, 247–264.

Hartnett H. E., Keil R. G., Hedges J. I. and Devol A. H. (1998) Influence of oxygen exposure time on organic carbon preservation in continental margin sediments. *Nature* **391**, 572–574.

Hastings R. H., Goñi M. A., Wheatcroft R. A. and Borgeld J. C. (2012) A terrestrial organic matter depocenter on a high-energy margin: the Umpqua River system, Oregon. *Cont. Shelf Res.* **39–40**, 78–91.

Hasvold Ø., Henriksen H., Mevar E., Citi G., Johansen B. Ø., Kjønigsen T. and Galetti R. (1997) Sea-water battery for subsea control systems. *J. Power Sources* **65**, 253–261.

Hedges J. I., Hu F. S., Devol A. H., Hartnett H. E., Tsmakis E. and Keil R. G. (1999) Sedimentary organic matter preservation: a

test for selective degradation under oxic conditions. *Am. J. Sci.* **299**, 529–555.

Hedges J. I. and Stern J. H. (1984) Carbon and nitrogen determinations of carbonate containing solids. *Limnol. Oceanogr.* **49**, 657–663.

Hee C. A., Pease T. K., Alperin M. J. and Martens C. S. (2001) Dissolved organic carbon production and consumption in anoxic marine sediments: a pulsed-tracer experiment. *Limnol. Oceanogr.* **46**, 1908–1920.

Holmes D. E., Bond D. R., O'Neil R. A., Reimers C. E., Tender L. M. and Lovley D. R. (2004) Microbial communities associated with electrodes harvesting electricity from a variety of aquatic sediments. *Microb. Ecol.* **48**, 178–190.

Hulthe G., Hulth S. and Hall P. O. J. (1998) Effect of oxygen on degradation rate of refractory and labile organic matter in continental margin sediments. *Geochim. Cosmochim. Acta* **62**, 1319–1328.

Ishii S., Shimoyama T., Hotta Y. and Watanabe K. (2008) Characterization of a filamentous biofilm community established in a cellulose-fed microbial fuel cell. *BMC Microbiol* **8**. http://dx.doi.org/10.1186/1471-2180-8-6.

Jørgensen B. B. (2006) Bacteria and marine biogeochemistry. In *Marine Geochemistry* (eds. H. D. Schulz and M. Zabel). Springer, pp. 169–206.

Jung S. and Regan J. M. (2007) Comparison of anode bacterial communities and performance in microbial fuel cells with different electron donors. *Appl. Microb. Cell Physiol.* **77**, 393–402.

Keil R. G., Hu F. S., Tsamakis E. C. and Hedges J. I. (1994) Pollen in marine sediments as an indicator of oxidation of organic matter. *Nature* **369**, 639–641.

Kiely P. D., Regan J. M. and Logan B. E. (2011) The electric picnic: synergistic requirements for exoelectrogenic microbial communities. *Curr. Opin. Biotechnol.* **22**, 378–385.

Kobayashi T., Koide O., Mori K., Shimamura S., Matsuura T., Miura T., Takaki Y., Morono Y., Nunoura T., Imachi H., Inagaki F., Takai K. and Horikoshi K. (2008) Phylogenetic and enzymatic diversity of deep subseafloor aerobic microorganisms in organics- and methane-rich sediments off Shimokita Peninsula. *Extremophiles* **12**, 519–527.

Lee C. (1992) Controls on organic carbon preservation: the use of stratified water bodies to compare intrinsic rates of decomposition in oxic and anoxic systems. *Geochim. Cosmochim. Acta* **56**, 3323–3335.

Lenk S., Arnds J., Zerjatke K., Musat N., Amann R. and Mußmann M. (2011) Novel groups of *Gammaproteobacteria* catalyse sulfur oxidation and carbon fixation in a coastal intertidal sediment. *Environ. Microbiol.* **13**, 758–774.

Leung K. M., Wanger G., Guo Q., Gorby Y., Southam G., Lau W. M. and Yang J. (2011) Bacterial nanowires: conductive as silicon, soft as polymer. *Soft Matter* **7**, 6617–6621.

Liu H., Cheng S. and Logan B. E. (2005) Power generation in fed-batch microbial fuel cells as a function of ionic strength, temperature and reactor configuration. *Environ. Sci. Technol.* **39**, 5488–5493.

Logan B. E., Hamelers B., Rozendal R., Schröder U., Keller J., Freguia S., Aelterman P., Verstraete W. and Rabaey K. (2006) Microbial fuel cells: methodology and technology. *Environ. Sci. Technol.* **40**, 5181–5192.

Lovley D. R. (2012) Electromicrobiology. *Annu. Rev. Microbiol.* **66**, 391–409.

Lovley D. R. and Chapelle F. H. (1995) Deep subsurface microbial processes. *Rev. Geophys.* **33**, 365–381.

Lovley D. R. and Phillips E. J. P. (1988) Novel mode of microbial energy metabolism: organic carbon oxidation coupled to dissimilatory reduction of iron or manganese. *Appl. Environ. Microbiol.* **54**, 1472–1480.

Margulies M., Egholm M., Altman W. E., Attiya S., Bader J. S., Bemben L. A., Berka J., Braverman M. S., Chen Y.-J., Chen Z., Dewell S. B., Du L., Fierro J. M., Gomes X. V., Godwin B. C., He W., Helgesen S., Ho C. H., Irzyk G. P., Jando S. C., Alenquer M. L. I., Jarvie T. P., Jirage K. B., Kim J.-B., Knight J. R., Lanza J. R., Leamon J. H., Lefkowitz S. M., Lei M., Li J., Lohman K. L., Lu H., Makhijani V. B., McDade K. E., McKenna M. P., Myers E. W., Nickerson E., Nobile J. R., Plant R., Puc B. P., Ronan M. T., Roth G. T., Sarkis G. J., Simons J. F., Simpson J. W., Srinivasan M., Tartaro K. R., Tomasz A., Vogt K. A., Volkmer G. A., Wang S. H., Wang Y., Weiner M. P., Yu P., Begley R. F. and Rothberg J. M. (2005) Genome sequencing in microfabricated high-density picolitre reactors. *Nature* **437**, 376–380.

Marsili E., Baron D. B., Shikhare I. D., Coursolle D., Gralnick J. A. and Bond D. R. (2008) *Shewanella* secretes flavins that mediate extracellular electron transfer. *PNAS* **105**, 3968–3973.

Mayer L. M. (1994) Surface area control of organic carbon accumulation in continental shelf sediments. *Geochim. Cosmochim. Acta* **58**, 1271–1284.

Mayer L. M., Jumars P. A., Bock M. J., Vetter Y.-A. and Schmidt J. L. (2001) Two roads to sparagmos: extracellular digestion of sedimentary food by bacterial inoculation versus deposit-feeding. In *Organism–Sediment Interactions* (eds. J. Y. Aller, S. A. Woodin and R. C. Aller). University of South Carolina Press, pp. 335–347.

McKee B. A., Aller R. C., Allison M. A., Bianchi T. S. and Kineke G. C. (2004) Transport and transformation of dissolved and particulate materials on continental margins influenced by major rivers: benthic boundary layer and seabed processes. *Cont. Shelf Res.* **24**, 899–926.

McNichol A. P., Lee C. and Druffel E. R. M. (1988) Carbon cycling in coastal sediments: 1. A quantitative estimate of the remineralization of organic carbon in the sediments of Buzzards Bay, MA. *Geochim. Cosmochim. Acta* **52**, 1531–1543.

Middelburg J. J. (1989) A simple model for organic matter decomposition in marine sediments. *Geochim. Cosmochim. Acta* **53**, 1577–1581.

Morford J. L. and Emerson S. (1999) The geochemistry of redox sensitive trace metals in sediments. *Geochim. Cosmochim. Acta* **63**, 1735–1750.

Morse J. W. and Berner R. A. (1995) What determines sedimentary C/S ratios? *Geochim. Cosmochim. Acta* **59**, 1073–1077.

Nealson K. H. (2010) Sediment reactions defy dogma. *Nature* **463**, 1033–1034.

Newman D. K. and Kolter R. (2000) A role for excreted quinones in extracellular electron transfer. *Nature* **405**, 94–97.

Nielsen L. P., Risgaard-Petersen N., Fossing H., Christiansen P. B. and Sayama M. (2010) Electric currents couple spatially separated biogeochemical processes in marine sediment. *Nature* **463**, 1071–1074.

Nielsen M. E., Reimers C. E., White H. K., Sharma S. and Girguis P. R. (2008) Sustainable energy from deep ocean cold seeps. *Energy Environ. Sci.* **1**, 584–593.

Nielsen M. E., Wu D. M., Girguis P. R. and Reimers C. E. (2009) Influence of substrate on electron transfer mechanisms in chambered benthic microbial fuel cells. *Environ. Sci. Technol.* **43**, 8671–8677.

Pfeffer C., Larsen S., Song J., Dong M., Besenbacher F., Meyer R. L., Kjeldsen K. U., Schreiber L., Gorby Y. A., El-Naggar M. Y., Leung K. M., Schramm A., Risgaard-Petersen N. and Nielsen L. P. (2012) Filamentous bacteria transport electrons over centimeter distances. *Nature* **491**, 218–221.

Prahl F. G., DeLange G. J., Scholten S. and Cowie G. L. (1997) A case of postdepositional aerobic degradation of terrestrial organic matter in turbidite deposits from the Madeira Abyssal Plain. *Org. Geochem.* **27**, 141–152.

Rabaey K., Boon N., Höfte M. and Verstraete W. (2005) Microbial phenazine production enhances electron transfer in biofuel cells. *Environ. Sci. Technol.* **39**, 3401–3408.

Rabaey K., Rodriguez J., Blackall L. L., Keller J., Gross P., Batstone D., Verstraete W. and Nealson K. H. (2007) Microbial ecology meets electrochemistry: electricity-driven and driving communities. *ISME J.* **1**, 9–18.

Raymond P. A. and Bauer J. E. (2001) DOC cycling in a temperate estuary: a mass balance approach using natural ^{14}C and ^{13}C. *Limnol. Oceanogr.* **46**, 655–667.

Reguera G., McCarthy K. D., Mehta T., Nicoll J. S., Tuominen M. T. and Lovley D. R. (2005) Extracellular electron transfer via microbial nanowires. *Nature* **435**, 1098–1101.

Reimers C. E., Girguis P., Stecher, III, H. A., Ryckelynck N., Tender L. M. and Whaling P. (2006) Microbial fuel cell energy from an ocean cold seep. *Geobiology* **4**, 123–136.

Reimers C. E., Stecher, III, H. A., Westall J. C., Alleau Y., Howell K. A., Soule L., White H. K. and Girguis P. R. (2007) Substrate degradation kinetics, microbial diversity, and current efficiency of microbial fuel cells supplied with marine plankton. *Appl. Environ. Microbiol.* **73**, 7029–7040.

Risgaard-Petersen N., Revil A., Meister P. and Nielsen L. P. (2012) Sulfur, iron-, and calcium cycling associated with natural electric currents running through marine sediment. *Geochim. Cosmochim. Acta* **92**, 1–13.

Røy H., Kallmeyer J., Adhikari R. R., Pockalny R., Jørgensen B. B. and D'Hondt S. (2012) Aerobic microbial respiration in 86-million-year-old deep-sea red clay. *Science* **336**(6083), 922–925. http://dx.doi.org/10.1126/science.1219424.

Rusch A., Hannides A. K. and Gaidos E. (2009) Diverse communities of active Bacteria and Archaea along oxygen gradients in coral reef sediments. *Coral Reefs* **28**, 15–26.

Ryckelynck N., Stecher, III, H. A. and Reimers C. E. (2005) Understanding the anodic mechanism of a seafloor fuel cell: interactions between geochemistry and microbial activity. *Biogeochemistry* **76**, 113–139.

Severmann S., McManus J., Berelson W. M. and Hammond D. E. (2010) The continental shelf benthic iron flux and its isotope composition. *Geochim. Cosmochim. Acta* **74**, 3984–4004.

Srikantha S., Marsili E., Flickinger M. C. and Bond D. R. (2007) Electrochemical characterization of *Geobacter sulfurreducens* cells immobilized on graphite paper electrodes. *Biotechnol. Bioeng.* **99**, 1065–1073.

Soetaert K., Herman P. M. J. and Middelburg J. J. (1996) A model of early diagenetic processes from the shelf to abyssal depths. *Geochim. Cosmochim. Acta* **60**, 1019–1040.

Sun M.-Y., Aller R. C., Lee C. and Wakeham S. G. (2002) Effects of oxygen and redox oscillation on degradation of cell-associated lipids in surficial marine sediments. *Geochim. Cosmochim. Acta* **66**, 2003–2011.

Tender L. M., Reimers C. E., Stecher, III, H. A., Holmes D. E., Bond D. R., Lovley D. R., Lowry D. A., Pilobello K. and Fertig S. (2002) Harnessing microbially generated power on the seafloor. *Nat. Biotechnol.* **20**, 821–825.

Thomson J., Jarvis I., Green D. R. H., Green D. A. and Clayton T. (1998) Mobility and immobility of redox-sensitive elements in deep-sea turbidites during shallow burial. *Geochim. Cosmochim. Acta* **62**, 643–656.

Uría N., Muñoz-Berbel X., Sánchez O., Muñoz F. X. and Mas J. (2011) Transient storage of electrical charge in biofilms of *Shewanella oneidensis* mr-1 growing in a microbial fuel cell. *Environ. Sci. Technol.* **45**, 10250–10256.

Wang Q., Garrity G. M., Tiedje J. M. and Cole J. R. (2007) Naive Bayesian classifier for rapid assignment of rRNA sequences into the new bacterial taxonomy. *Appl. Environ. Microbiol.* **73**(16), 5261–5267.

Wheatcroft R. A., Goñi M. A., Richardson K. N. and Borgeld J. C. (2013) Natural and human impacts on centennial sediment accumulation patterns on the Umpqua River margin, Oregon. *Mar. Geol.* **339**, 44–56.

White H. K., Reimers C. E., Cordes E. E., Dilly G. F. and Girguis P. R. (2009) Quantitative population dynamics of microbial communities in plankton-fed microbial fuel cells. *ISME J.* **3**, 635–646.

Zhao Y., Ren N. and Wang A. (2008) Contributions of fermentative acidogenic bacteria and sulfate-reducing bacteria to lactate degradation and sulfate reduction. *Chemosphere* **72**, 233–242.

Associate editor: Marc Norman